Effect of Steels on the Purity of Molten Mg Alloys

Tao Chen, Xiao Xiong, Yuan Yuan,* Aitao Tang,* Dajian Li, Andrej Atrens, and Fusheng Pan

Tooling materials used in the synthesizing of Mg alloys can introduce impurities, which can severely degrade the anticorrosion properties for the final Mg products. To address this issue, this work analyze the purity of molten Mg alloys AZ91D and AM50A in contact with three commonly used steels: 20#, H13, High-CrNi (022Cr25Ni7Mo4N) for different durations at various temperatures. Interactions between alloying elements and impurity elements are analyzed combining the thermodynamic and kinetics. Results show that low holding temperatures (below 680 °C) can significantly reduce the amount of introduced impurities. H13 steel has the smallest effect on the final purity of the molten Mg alloys and the presence of Cr can inhibit the dissolution of Fe into molten Mg alloys.

1. Introduction

Magnesium (Mg) alloys have received extensive attention in industrial applications due to their low density, low modulus of elasticity, high-specific strength, and high-specific stiffness.[1–4] However, the low-temperature formability[5] and low corrosion resistance[6–8] of Mg alloys limit their large-scale applications.

Many researches have indicated that the impurity elements, Fe, Ni, Cu, Co, in Mg alloys can strongly increase their corrosion rate,[9–11] and also severely deteriorate the mechanical[12–14] and damping properties.[15] When the impurities content in

alloys exceeds the "tolerance limit" (10 ppm magnitude), the corrosion rate of Mg alloys will be exponentially accelerated.[16] Therefore, it is of great significance to strictly control the purity of the Mg alloys, especially the purity of the molten alloys before casting.

Unfortunately, it is almost impossible to completely avoid these impurities during the production of Mg alloys. First, during Mg-metal smelting, no matter whether the Pidgeon method or the electrolytic magnesium method is used, there are always some impurities picked up from the raw materials. Second, these elements existing in the steel tools and steel crucibles can be dissolved in the molten Mg alloys during the melting process.[17–20]

The purification of the molten Mg and Mg alloys has been studied extensively.[21–24] However, the effect resulting from defined tools on the Mg alloys production is rarely studied.[19,25] Scharf and Ditze[19] studied the interaction layers between AZ91 and AS31 with steel crucibles. The dissolution of iron, low-carbon steel, and SUS316 (11wt% Ni, 17wt% Cr, remainder Fe) crucibles in commercial pure molten Mg was investigated by Taninouchi et al.[25] However, the influence of the types of used steels on the purity of molten Mg alloys has not been studied. Only by understanding the specific impact of elements coming from the tooling materials on the purity of molten Mg alloys can assure the purity of Mg alloys.

This work aims to quantitatively determine the effect of tooling materials on the purity of Mg alloys melt. The most commonly cast Mg alloys, AZ91D, and AM50A, were studied. Three types of common tooling materials used in the production of Mg alloys: 20# steel, H13 steel, High-CrNi (022Cr25Ni7Mo4N) steel, were studied. Low carbon steel (here 20#) is the most common material used as the crucible materials for the Mg alloys synthesis. H13 steel is commonly used for Mg alloys casting molds. High-CrNi heat-resistant steel is commonly seen for the reduction tank in the Pidgeon process. The interactions between these tooling materials and Mg alloys were pre-evaluated using the Thermo-Calc 2019 software[26] based on the TCMG5 thermodynamic database. The influence of tooling materials on the purity of molten Mg alloys was experimentally studied using the liquid–solid diffusion method. What is more, the thermodynamic information is very important for the effective alloy design as well as the prediction of the distribution of impurities in alloys.[27–29] However, there is little thermodynamic information on the dilute part of the phase diagram. The currently measured content of Fe, Ni, Cr

T. Chen, X. Xiong, Prof. Y. Yuan, Prof. A. Tang, Prof. F. Pan
State Key Laboratory of Mechanical Transmissions
College of Materials Science and Engineering
Chongqing University
Chongqing 400044, China
E-mail: yuanyuan17@cqu.edu.cn; tat@cqu.edu.cn

T. Chen, X. Xiong, Prof. Y. Yuan, Prof. A. Tang, Prof. F. Pan
National Engineering Research Center for Magnesium Alloys
College of Materials Science and Engineering
Chongqing University
Chongqing 400044, China

Dr. D. Li
Institute for Applied Materials – Applied Materials Physics (IAM-AWP)
Karlsruhe Institute of Technology
Karlsruhe 76344, Germany

Prof. A. Atrens
School of Mechanical and Mining Engineering
Advanced Materials Processing and Manufacturing
The University of Queensland
St Lucia, QLD 4072, Australia

The ORCID identification number(s) for the author(s) of this article can be found under https://doi.org/10.1002/adem.202000338.

**ADVANCED
SCIENCE NEWS**

www.advancedsciencenews.com

**ADVANCED
ENGINEERING
MATERIALS**

www.aem-journal.com

in liquids is also valuable experimental data for the revision of current thermodynamic database.

2. Calculation and Experimental Methods

2.1. Thermodynamics Calculation and Prediction

TCMG5 database and COST507 database were used to predict the effect of steels on the purity of molten Mg alloys using Thermo-Calc 2019a software for the calculation. The two extreme conditions of CALPHAD-type calculations were considered in this work. One is the thermodynamics equilibrium simulation, which assumed that the whole system is considered to be at thermodynamics equilibrium state. This equilibrium calculation was applied for the solubility calculation. The other is the Scheil solidification mode, which assumed that the complete diffusion occurred in liquid and no diffusion in the solid phases. This Scheil simulation was used to assess the final state of alloys. According to the literature collection, there is no (experimental or theoretical) report about the solubility of Fe in the Mg-Al-Zn or Mg-Al-Mn system. Also, there have been no full thermodynamic assessments of the related Fe-Mg-Al-Zn, Ni-Mg-Al-Zn, Cr-Mg-Al-Zn systems conducted. Hence, the current evaluations in this work are just based on the extrapolations from subsystems and compared with the obtained experimental data.

2.2. Experimental Methods

MgO crucibles (98%) were used in the melting experiments. Different types of steel sheets were inserted into the molten Mg alloys, compositions shown in **Table 1**, and allowed to react with the molten Mg alloys at five holding temperatures of 650, 680, 720, 760, and 780 °C for holding periods of 1, 2, 4 and 6 h, as shown in **Figure 1**a. All alloys were melted in a well-type resistance furnace with the temperature controlled by a thermocouple to ± 5 °C under protection gas of 99.5 vol% CO_2 and 0.5 vol% SF_6. The semi-in-situ sampling method was developed by our group. During the holding process, as shown in Figure 1b, a small amount of alloy (3–10 mL) was taken from the melt by a 10 mm inner diameter copper tube (99.9 wt% Cu) at the defined holding period. Also, the liquid in the copper tube was quenched quickly in cold water. Subsequently, these samples in the copper tubes were taken out, polished and analyzed by inductively coupled plasma–optical emission spectrometry (ICP-OES, Optima 8300).

After a 6 h maximum holding period, the molten alloys were slowly cooled to room temperature in the furnace. The interface of Mg alloys ingots with steel sheets was sliced and polished using the standard metallographic treatment. Finally, these
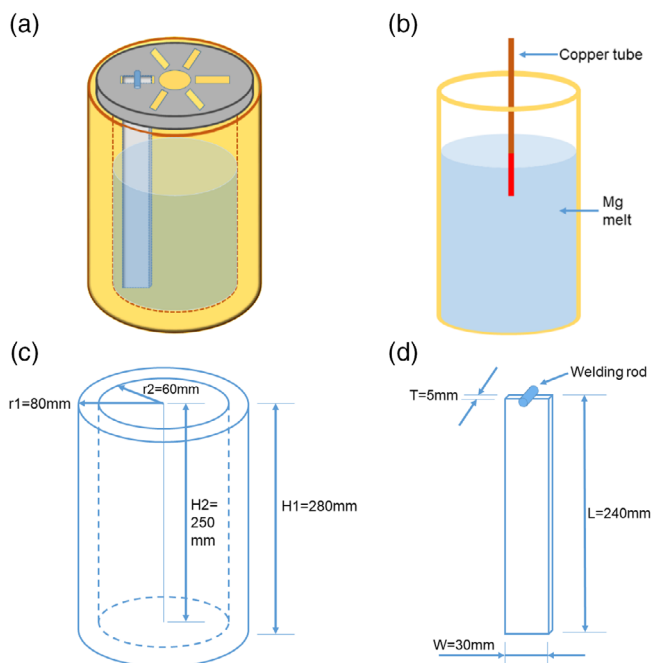

Figure 1. a) Schematic diagram of the melting device; b) Schematic diagram of sampling; c) Schematic diagram of crucible; d) Schematic diagram of steel sheets.

samples were analyzed using a scanning electron microscope (SEM, TESCAN VEGA3 LMH SEM) and the concentration profiles along the interface were measured using energy-dispersive X-ray spectroscopy (EDS, OXFORD INCA energy 350).

3. Results

Figure 2 shows the calculated results of the thermodynamic equilibrium solubility of Fe and Ni in the investigated Mg alloys liquid phase. The solubility of Fe in pure Mg liquid phase was 312 ppm (weight fraction was used throughout this work) at 700 °C. For AM50A containing 4.77 wt% Al and 0.41 wt% Mn, the solubility of Fe at 700 °C in Mg liquid phase decreased to 7 ppm. As shown in Figure 2b, Ni has a very large solubility in molten Mg where the eutectic reaction of Mg–Ni occurs at the point of 23 wt% Ni. The solubility of Ni in Mg-4.77-0.41Mn, Mg-4.77Al, Mg-9.41Al-0.72Zn, and Mg-9.41Al in 850 °C was 2120, 2082, 1952, 1972 ppm (in weight fraction), separately.

With the steel sheet staying in the molten AZ91D, the elements in the sheet were gradually solved into the molten alloys. **Figure 3** shows the measured content of dissolved Fe in the molten AZ91D. The AZ91D was in contact with the 20# steel, H13 steel, and High-CrNi steel, separately. The values of Fe content obtained from different positions of the molten alloys were all plotted in the graphs. It is seen that if considering the experimental error range, the values of Fe content obtained from different positions do not show much difference. It means the molten alloys during the holding period were being almost stable and there was no clear dynamic turbulent or noise in the temperature field.
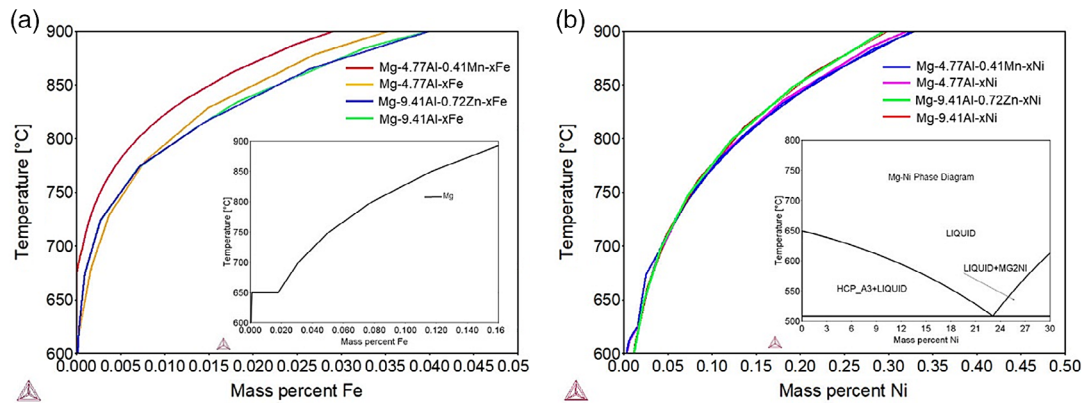
Table 1. The chemical composition of the investigated Mg alloys AZ91D and AM50A.

Mg alloy	Chemical position [wt%]								
	Mg	Al	Zn	Mn	Fe	Cu	Si	Ni	Etc.
AZ91D	Bal.	9.41	0.72	0.22	0.0015	0.0003	0.0049	0.0007	≤0.2
AM50A	Bal.	4.77	0	0.41	0.0013	0.0001	0.0021	0.0005	≤0.05

**ADVANCED
SCIENCE NEWS**

www.advancedsciencenews.com

**ADVANCED
ENGINEERING
MATERIALS**

www.aem-journal.com

Figure 2. a) The calculated Fe solubility in the investigated molten Mg alloys; b) The calculated Ni solubility in the investigated molten Mg alloys.

With the increase in holding temperature, the content of Fe in molten Mg alloys increased. With the prolonged holding time, the content of Fe in molten Mg alloys increased initially and then gradually approached to stable values. As shown in Figure 3, in general, the content of Fe in the AZ91D increased quickly in the first 1 h, and then the slopes of the lines decreased after the first 1–2 h. Finally, the content of Fe in AZ91D approached to stable values after 4 h of holding period, and it is seen the further increment of the holding period did not change much of the content of Fe in molten alloys. It can be assumed that the obtained Fe content in the molten alloys in this work reached the equilibrium maximum solubility in the corresponding alloys melt at the investigated temperature after the full holding/diffusion period, 6 h in this case. Furthermore, the content of Fe in AZ91D melt contacting with 20# steel was significantly higher than that in AZ91D melt contacting with H13 steel and also higher than that in AZ91D melt contacting with High-CrNi steel. For example, the stable Fe content at 650 °C was around 120 ppm in the melt contacting with 20# steel, around 40 ppm in the melt contacting with H13 steel and in the melt contacting with High-CrNi steel. The red dash lines in Figure 3 show the calculated equilibrium solubility of Fe in the AZ91D melt at the defined temperature based on the TCMG5 thermodynamic database. As shown in Figure 3, the experimental stable values of Fe content in melt were much higher than those calculated equilibrium values. For example, the calculated equilibrium Fe solubility in AZ91D at 680 °C was only around 10 ppm, much lower than the measured values, around 140 ppm of Fe in the melt which was contacting with 20# steel.

Figure 4 shows the images of interfaces of alloys contacting with steels and the concentration profiles along the interface scanned by the EDS. As shown in Figure 4, the interfacial diffusion layer at 680 °C was around 15 μm and at 760 °C around 30 μm, separately, as regions marked by the dash lines.

The curves of Fe content in the molten AM50A contacting with different types of sheets are shown in **Figure 5**, with variations in holding temperatures and holding periods. The behavior of solution of Fe in AM50A melt shown in Figure 5 is similar as that in AZ91D melt shown in Figure 3. It is seen with the increase in holding time, the Fe content in the melt was increasing sharply in the first-hour holding period and then approach to

stable values after 4 h holding period. The content of Fe in the AM50A melt contacting with 20# steel was also much higher than that contacting with H13 steel and that contacting with High-CrNi steel.

Figure 6 shows that, after 6 h holding period, a small amount of Cr, coming from steel sheets, was dissolved into the molten AM50A and AZ91D. The amount of Cr dissolved in AM50A was smaller than that dissolved in AZ91D. At 650 °C, the Cr content in melt increased slightly with the holding period prolonging, and was around 10 ppm in the final molten AM50A and around 20 ppm in the final molten AZ91D, separately. When the holding temperature exceeded 720 °C, the Cr content in the AZ91D and AM50A melt was significantly increased. When the temperature reached 780 °C, the Cr content in the melt contacting with High-CrNi steel was still increased sharply even after 6 h holding period, reaching 100 ppm. The calculated values of Cr content in the pure molten Mg were compared with the experimental values of Cr content in the AZ91D and AM50A alloys melt. Different with the case of Fe, the Cr content in the melt at high temperature was continuously increasing along the full holding period. Furthermore, the Cr content in the AZ91D melt was higher than that in the AM50A melt.

Figure 7 shows the Ni content in molten AZ91D and AM50A in contact with High-CrNi steel. With the holding temperature at 650 °C, the Ni content in the AM50A melt contacting with High-CrNi steel did not change much with the increasing holding period. With the holding temperature at 720 °C, the Ni content in melt increased significantly with the extension of the holding time and did not reach stable values after 6 h holding period. With the holding temperature increased to 780 °C, the content of Ni in the melt increased rapidly along the full holding period.

4. Discussion

4.1. The Equilibrium Solubility of Fe, Cr, Ni in Mg Liquid Phase and Possible Presented State of Impurities in the Solidified Alloys

The presented phase boundaries in Figure 2 indicate that the presence of Mn in the melt can reduce the solubility of Fe in liquid phase and the Zn addition in Mg alloys does not cause
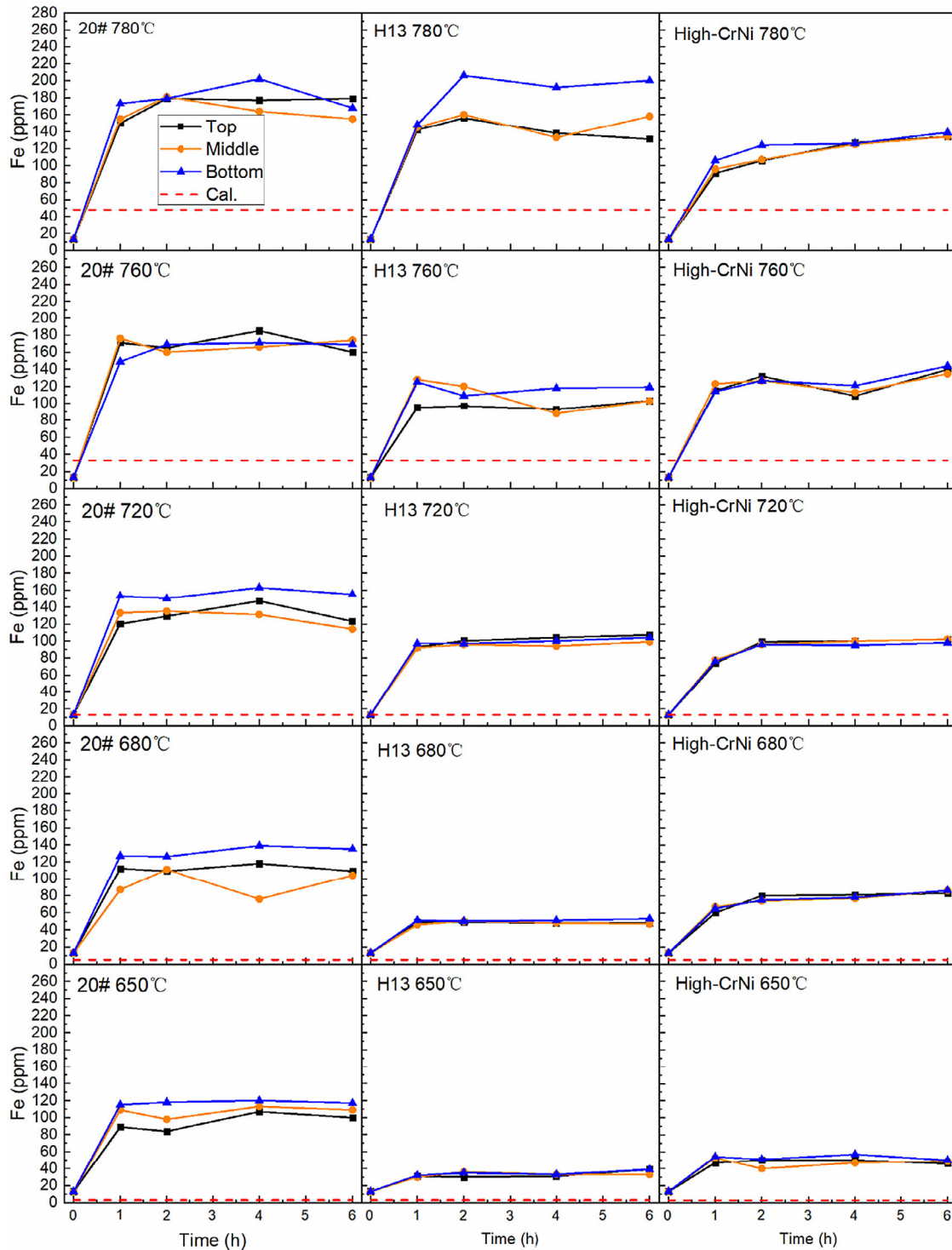
Cal. : The solubility of Fe in Mg-9.41Al-0.72Zn-0.22Mn calculated by TCMG5

Figure 3. The Fe content in molten AZ91D in contact with 20# steel, H13 steel, and High-CrNi steel, separately. Cal.: The solubility of Fe in Mg-9.41Al-0.72Zn-0.22Mn calculated by TCMG5.

much difference in the solubility of Fe in melt. When these alloys were cooled to the solid state, part of the Fe atoms can be dissolved in the α(Mg) phase within the solubility range, which is below 1 ppm at 464 °C for AZ91D (Mg-9.41Al-0.72Zn-0.22Mn) (just below the equilibrium solidification temperature) and the excess Fe atoms can be combined with other atoms to form
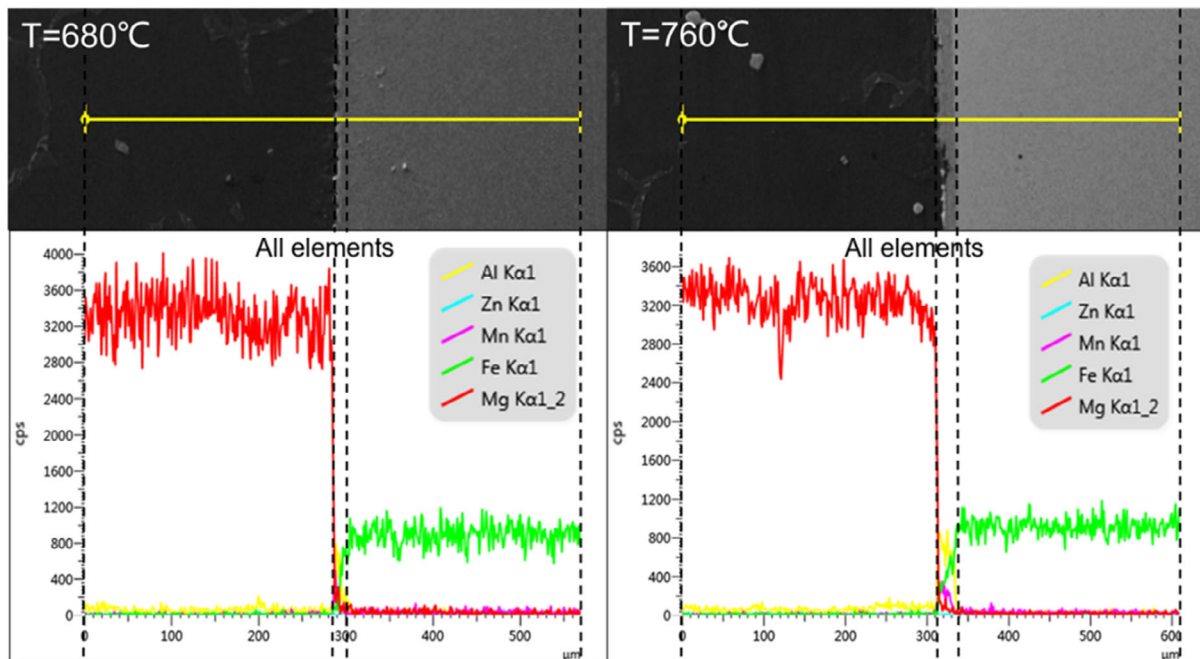
Figure 4. Composition profile of the interfaces between AZ91D Mg alloy and 20# steel sheet at 680, 760 °C after 6 h of diffusion.

compounds. Commonly, Bcc(Al, Mn, Fe), Al_5Fe_2, $Al_8(Mn, Fe)_5$ phase can be found in the final solidified alloys depending on the whole composition of alloys and the casting condition.

There is no Cr element in the current TCMG5 database. Furthermore, there is also little research on the solubility of Cr in molten Mg alloys.[30,31] Ansara et al.[32] assessed the Cr–Mg system, which is included in the COST507 database. According to the calculations based on COST507 database, the solubility of Cr in Mg liquid phase at 700 °C is 11 ppm. The solubility of Cr in α(Mg) phase is 3 ppm at 650 °C. The excess of Cr atoms is presented as α(Cr) in the final solidified alloys.

The published Mg–Ni phase diagram shows a deep eutectic reaction at 23 wt% Ni at 512 °C.[33] However, according to the calculations using current available database, the Al addition in Mg–Ni alloys has a strong effect on the solution and phase transformation, compared with that of binary Mg–Ni system. For example, with 5 wt% Al added, Bcc(Al, Ni) phase can be precipitated in Mg alloys melt when Ni content exceeded the solubility. The formation of Al–Ni compounds dramatically decreased the solubility of Ni in liquid phase, which can have a strong inhibit effect on the dissolution of Ni from steel to the Mg alloy melt. However, it should be noted, as shown in Figure 2b, that the line of the solubility of Ni in Mg-4.77Al and that in Mg-9.41Al cross each other. What is more, He et al.'s results[34] show that no compound existed in the Mg-rich corner at 700 °C of Mg-Al-Ni isothermal cross section. Therefore, the thermodynamic data of Mg-Al-Ni system needs further investigation. The excess Ni impurity may be presented as Bcc(Al, Ni) in the final solidified alloy for Mg–Al-based alloys.

According to the aforementioned analysis, the solubility of Fe, Cr, and Ni in the liquid phase is around one or even two orders of magnitude than the solubility of Fe, Cr, and Ni in the α(Mg)

phase. In the solid state, the excess impurities can be combined with other elements and form Al–Fe, Al–Ni compounds, or even maybe elementary substance, such as α(Cr), in the final solidified alloy. The formed precipitates containing impurities, usually with high corrosion potential, can result in strong galvanic corrosion when they are contacting with α(Mg) phase. The presence of these precipitates can severely deteriorate the corrosion properties of Mg alloy. As reported in literature,[35] there are tolerance limit values for these impurities. Hence, it is significantly important to strictly control the content of impurities in Mg alloys.

4.2. Effect of 20# Steel, H13 Steel, and High-CrNi Steel on the Fe Dissolution in Molten AZ91D

As shown in Figure 3, for all cases, the obtained content of Fe in the melt contacting with various types of steels was much higher than that of the solubility values calculated using the TCMG5 database. Here the involved system is Mg-Al-Mn-Zn-Fe quinary system. The multi-element dissolved in the liquid phase can have a strong effect on the solubility of the specific element. Current thermodynamic calculations were based on the current available TCMG5 database, where the calculations related to high order system are probably just extrapolations from subsystems. Nevertheless, the little literature investigations on the dilute part of phase diagram make the current database have a low precision, or in other words, a low reliability in the dilute part. The multi-elements simultaneously dissolved in one phase can have complex effect on the solution of phase. In some cases, the solubility of element B dissolved in primary A phase can be inhibited by the third element; for example, Ti and La can decrease the dissolution of Fe in Al-Sn-Si system.[36,37] But the multi-elements simultaneously dissolved in one phase can also result in a big
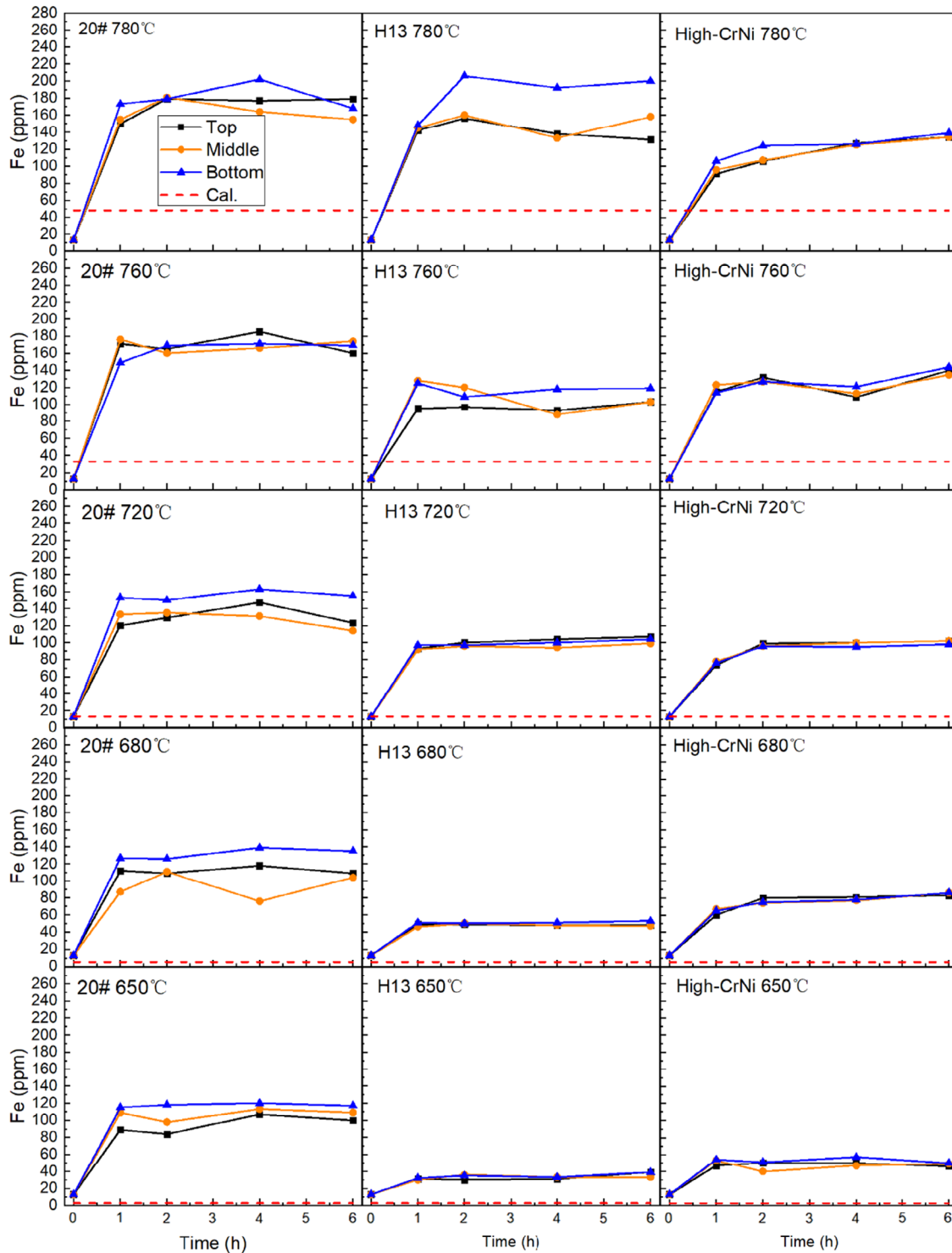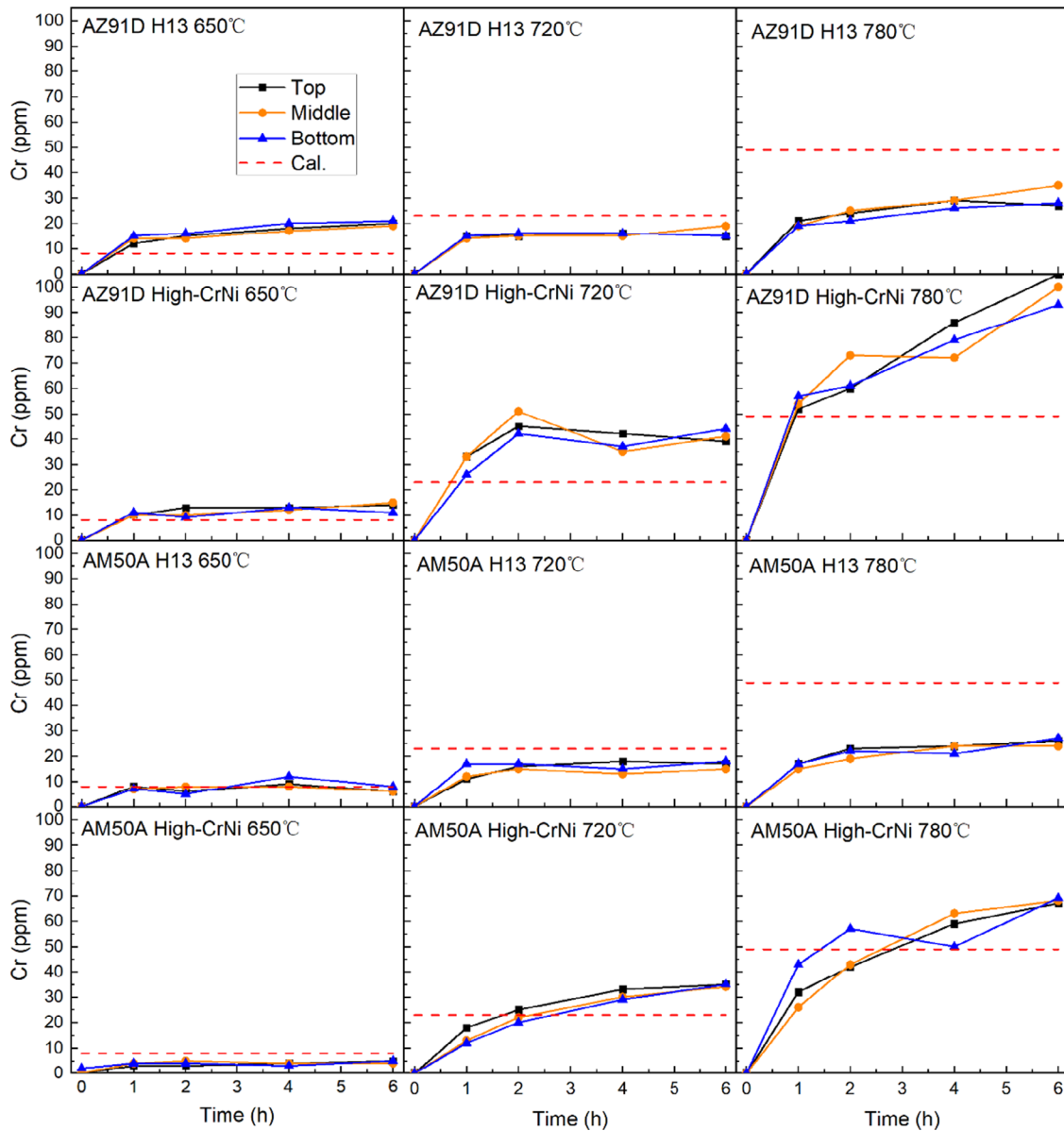
Cal. : The solubility of Fe in Mg-4.77Al-0.41Mn calculated using TCMG5 thermodynamic database

Figure 5. The Fe content in molten AM50A in contact with 20# steel, H13 steel, and High-CrNi steel, separately. Cal.: The solubility of Fe in Mg-4.77Al-0.41Mn calculated using TCMG5 thermodynamic database.

disorder entropy, which benefits the decrease in the energy and as a result, may increase the solubility of elements in solution phase. According to current thermodynamic data, the solubility

of Fe in AZ91 is only around 4 ppm at 650 °C. However, after many efforts from different researchers, the Fe content in final AZ91 alloys is still much higher than 10 ppm after different

ADVANCED
SCIENCE NEWS

www.advancedsciencenews.com

ADVANCED
ENGINEERING
MATERIALS

www.aem-journal.com

Cal.: The solubility of Cr in Mg calculated using COST507 database

Figure 6. The Cr content in molten AZ91D and AM50A in contact with H13 steel, separately. Cal.: The solubility of Cr in Mg calculated using COST507 database.

purification processes.[24] In another way, Liu et al.[10] corrected the tolerance limit value of impurities in Mg alloys with phase diagram. He suggested the tolerance level corresponds to the minimum content of Fe in cast Mg alloys for which no bcc crystal structure phase precipitates from the melt before final solidification. The reported tolerance limit of Fe for AZ91 is $0.032 \times Mn$.[35] For this work, the value is $0.21 \times 0.032 \approx 70$ ppm, which is close to our experimental values, where the Fe content at $650\,°C$ is around 100 ppm.

The content of Fe in the molten Mg alloys in contact with 20# steel were higher than that in the alloys in contact with H13 steel and that in contact with the High-CrNi steel. **Table 2** indicates that the main difference of these three types of steels

was the Cr content in the steel. The simultaneous dissolution of Cr into the melt decreased the dissolution of Fe in the melt.

As shown in Figure 3, the Fe content at different locations of the melt all increased with the increasing diffusion time. However, Figure 3 shows that the content of Fe at the bottom of melt was slightly higher than that at the top in some cases. Although there was no mechanical stirring, there were probably some small convections coming from the slight fluctuations of temperature. During the long-time diffusion process, the melt was not in full stable state, and the supersaturated Fe in some places settled down to the bottom of the crucible, which made an increasing aggregation of iron-containing precipitates in the bottom of the melt.
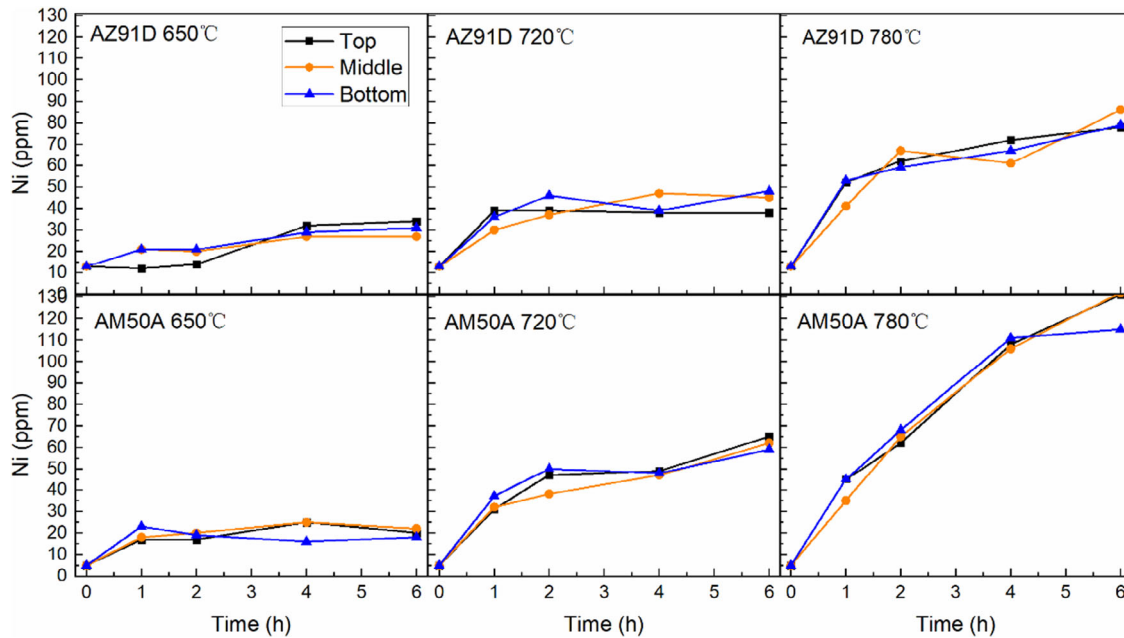
**ADVANCED
SCIENCE NEWS**

www.advancedsciencenews.com

**ADVANCED
ENGINEERING
MATERIALS**

www.aem-journal.com

Figure 7. The Ni content in molten AZ91D and AM50A in contact with High-CrNi steel. Note: The calculated Ni solubility is too big compared with the measured content of Ni in melt, around several hundred ppm, as shown in Figure 2b. Hence, the calculated Ni solubility is not presented in this figure.

Table 2. The chemical composition of the used steels.

Steel	Chemical position [wt%]								
	Fe	C	Si	Mn	Cr	Mo	Cu	Ni	N
20#	Bal.	0.20	0.35	0.50	0.20	–	0.20	0.20	–
H13	Bal.	0.36	0.82	0.36	4.95	1.40	–	–	–
022Cr25Ni7Mo4N	Bal.	0.03	0.80	1.20	25.0	4.00	0.50	7.00	0.25

Figure 3 shows that the selection of the melting temperature has a big impact on the final purity of the Mg alloys. The Fe content in the Mg alloys melted at 780 °C was more than double that in the Mg alloys melted at 650 °C. For example, within the group of alloys contacting with the High-CrNi steel, the Fe content was 60 ppm at 650 °C and 223 ppm at 780 °C, separately.

According to Figure 4, the thickness of the interfacial diffusion layer was increased with the increased melting/diffusion temperature. The main elements in the diffusion layers were Fe, Al, and Mn. As the steel sheets were in solid state, it was difficult for the Al and Mn atoms to diffuse deep into the steel from the molten Mg. The Al and Mn atoms were enriched on the surface of the 20# steel sheets. The Fe atoms from the steels diffused into the molten Mg alloys. According to the final Fe content in the alloy, the 20# steel can introduce more Fe atoms in the alloy. Therefore, in the production process of AZ91, it is recommended not to use a 20# steel, and the holding time should be kept short.

4.3. Effect of 20# Steel, H13 Steel, and High-CrNi Steel on the Fe Dissolution in Molten AM50A

The effect of 20#, H13, and High-CrNi steel on the Fe dissolution in molten AM50A is shown in Figure 5. The impurity content was compared with the calculated solubility. When the melting temperature is 650 °C, with the extension of the holding time, the Fe content in the AM50A melt contacting with H13 steel is small, around 40 ppm, but the Fe content in the AM50A melt contacting with 20# steel and that contacting with High-CrNi steel is much bigger, around 100 ppm in the melt contacting with 20# steel and around 50 ppm in the melt contacting with High-CrNi steel, separately. It indicates that H13 steel has the smallest impact on the purity of AM50A melt at this temperature.

Compared with Figure 3 and 5, no matter which kind of steel is used, under the same holding time, the Fe content in AM50A melt is lower than that in AZ91D melt. This difference can be attributed to the presence of more Mn in AM50A. Wang et al.[38] investigated the thermodynamic data of the Mg-Mn-Fe system and found the solubility of Fe in liquid Mg was reduced by alloying with Mn. In Section 4.1, the calculated results also show that Mn in the melt can reduce the solubility of Fe in liquid Mg alloys. AM50A contains more Mn than AZ91D (0.41 wt% vs 0.22 wt%), which can decrease the dissolution of Fe in AM50A. In general, the dissolution behavior of Fe in the two alloys was similar.

4.4. Effect of H13 and High-CrNi Steels on the Cr Dissolution in Molten AZ91D and AM50A

Cr is a common alloying element in steels. Figure 6 shows that Cr diffused into the Mg alloys melt when the Mg alloys melt was in contact with H13 and High-CrNi steels. As shown in Figure 6, after 6 h holding time, a small amount of Cr was dissolved into the molten Mg alloys melt. The Cr content in AM50A and AZ91D was less than 120 ppm below 780 °C. At high temperatures, High-CrNi steel can have a significant

**ADVANCED
SCIENCE NEWS**

www.advancedsciencenews.com

**ADVANCED
ENGINEERING
MATERIALS**

www.aem-journal.com

effect on the content of Cr in Mg alloys melt. This may be attributed to the Cr concentration in the used steel, where the Cr content in High-CrNi steel is five times of that in H13 steel.

Macroscopically, the Cr content in AM50A melt was, in general, a little smaller than that in AZ91D melt. Unfortunately, there is no thermodynamic information that can evaluate the effect of Al, Zn, Mn on the solubility of Cr in Mg alloys. Considering the similarity of Fe and Cr elements, this may be attributed to higher Mn content in AM50A which inhibited the dissolution of Cr in the melt as the similar cases of dissolution of Fe in these two alloys. What is more, the experimental results of Cr in alloys are close to the calculated solubility of Cr in pure Mg. This proves that the influence of alloying elements on the solubility of Cr is not as great as that of Fe and Ni.

4.5. Effect of High-CrNi Steel on the Ni Dissolution and Diffusion in Molten AZ91D and AM50A

Nickel is a harmful element for the corrosion resistance properties of Mg alloys. Only with a small amount Ni (in ppm grade) in the alloy, the corrosion properties of Mg alloys can be greatly deteriorated.[39,40] Figure 7 shows the dissolution behavior of Ni in the alloys. According to calculation using TCMG5 database, when the temperature is 650, 720, 780 °C, the solubility of Ni in AZ91D is 225, 539, 1024 ppm, respectively, and the solubility of Ni in AM50A is 204, 543, 1064 ppm, respectively. The calculated values of the solubility of Ni in the Mg alloys are much higher than the measured Ni content in the melt after 6 h of diffusion between steels and Mg alloys melt in this work. As shown in Figure 7, the Ni content was continuously increasing with the prolonging diffusion time and did not reach a stable value after 6 h diffusion period. That means, the Ni dissolution in the corresponding melt has not reached a stable state in this work. The reason could be attributed to the big solubility of Ni in the liquid phase, the small amount Ni content in the steels and as well, possible, the low diffusion rate of Ni. The contamination of Ni coming from High-CrNi steel to Mg alloys melt is very sensitive to temperature, in which the diffusion rate, which is varied with temperature, should be the main factor.

Furthermore, as shown in Figure 7, the dissolution of Ni content in the AZ91D melt in limited diffusion period was smaller than that in the AM50A melt. As the final equilibrium values were not reached in this work, the kinetics should be the main factor for this difference; some alloying elements may inhibit the dissolution and diffusion of Ni in the melt. Combined with the previous thermodynamic predictions in Section 4.1, it could be speculated that the Al element in the melt can inhibit the dissolution of Ni in the Mg alloys melt. Tathgar[41] measured the solubility of Ni and Fe in molten Mg–Al in the composition range of 0.3–9.4 wt% Al and temperature range of 650–900 °C, and showed the same tendency, where the Ni content in alloys decreased from 1.70 to 0.6 wt% as the Al content increased from 0.63 to 8.9 wt% after 20 h diffusion at 800 °C.

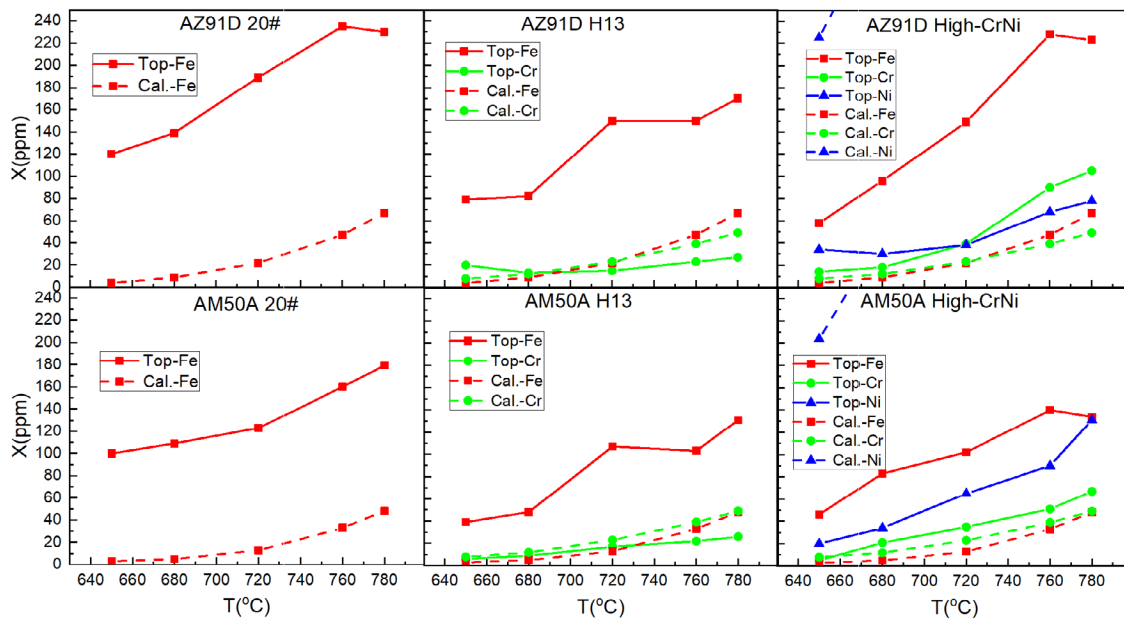### 4.6. General Discussions about the Effect of Tooling Materials on the Purity of the Synthesized Mg Alloys

In this work, first, currently available TCMG5 database was used to calculate the Fe and Ni solubility in the molten Mg alloys. Second, the effect of low-carbon steel, H13 steel, and High-CrNi steel in the melt on the final purity of AZ91D and AM50A melt was systematically investigated.

According to the thermodynamic predications, several points can be concluded here, which are consistent with our experimental results, although exactly different values presented: 1) Mn decreases the solubility of Fe in Mg-based liquid phase; 2) Al decreases slightly the solubility of Ni in Mg-based liquid phase; 3) The solubility of Fe in AZ91D melt was larger than that in AM50A melt.

Figure 8 shows the impurity content in the upper part of the melt after 6 h holding time, and the calculation results were also included for comparison. Unwanted impurities, such as Fe, Ni, Cr, can be easily diffused and dissolved to Mg alloys melt from tooling materials; here the steels were used. As described in Section 4.1, the corrosion rate could increase exponentially with the impurity content increase when the impurity content exceeds the "tolerance limit".[16] The tolerance limit values for AZ91 are: Fe ≤ 0.032 Mn, Ni ≤ 10 ppm, reported by Reichek et al.[35]. If the impurities content in AZ91 can be controlled under the tolerance, the salt spray corrosion performance of gravity cast AZ91 can be similar to that of the carbon steel or 380 die-cast Al alloy.[35] Froats et al.[42] found that the corrosion rate of AZ91 could be increased from 0.15 to 14.8 mm year^{-1} if Fe content increased from 19 to 160 ppm. Therefore, the strict control of the impurity content, even in ppm or 10*ppm order of magnitude, is still quite important for the performance of Mg alloys.

Figure 8 shows that the contaminations from tooling steels were small when the holding temperature is below 680 °C. With the temperature increasing above 720 °C, the impurities content in the final Mg alloys melt was quite big even though the holding time was limited in 1 h.

The total amounts of impurity content from steels in the melt are listed in **Table 3** (The Cr and Ni content in melt contacting with 20# steel and the Ni content in melt contacting with H13 steel were not measured in this work as the content of these elements in the related steels are quite small). As shown in Figure 8, when the melt was contacting with 20# steel, the content of Fe coming from the steel, was higher compared with that in the melt contacting with H13 steel and that in the melt contacting with High-CrNi steel. Table 3 shows the presence and dissolution of Cr in the melt probably have an inhibitive effect on Fe dissolution in melt. There is no thermodynamic data about the ternary systems of Mg-Fe-Ni-Cr. The dissolution behavior of elements coming from SUS316 crucibles in commercial pure Molten Mg at 800–1050 °C was investigated by Taninouchi et al.[25] Taninouchi et al.[25] reported Fe in stainless steel (or the altered layer at its surface) probably decreases other impurities, such as Cr and Ni diffusing to the alloys. Considering the similarity of Fe, Cr, Ni, the diffusion and solution of these three elements in the melt may affect each other. The further addition of Ni into Cr-containing Mg alloys showed no obvious influence on

ADVANCED
SCIENCE NEWS

www.advancedsciencenews.com

ADVANCED
ENGINEERING
MATERIALS

www.aem-journal.com

Top-X(X=Fe; Cr; Ni): The content of X element in the top part of the melt after 6-hour diffusion of steel sheets in the melt.

Cal.-Fe: The solubility of Fe in AZ91D or AM50A calculated by TCMG5

Cal.-Cr: The solubility of Cr in Mg calculated by COST507

Cal.-Ni: The solubility of Ni in AZ91D or AM50A calculated by TCMG5

Figure 8. Experimental and calculated solution of X(X = Fe/Cr/Ni) in molten AZ91D and AM50A. Top-X(X = Fe; Cr; Ni): The content of X element in the top part of the melt after 6 h diffusion of steel sheets in the melt. Cal.-Fe: The solubility of Fe in AZ91D or AM50A calculated by TCMG5; Cal.-Cr: The solubility of Cr in Mg calculated by COST507. Cal.-Ni: The solubility of Ni in AZ91D or AM50A calculated by TCMG5.

the Fe dissolution because the diffusion potentials of each element can be changed dependent on the composition gradient of the interface of melt/steel sheet.

As shown in Table 3, at 650 °C, the total impurities content in the Mg alloys melt contacting with H13 steel was the lowest compared with that in melt contacting other two types of steels. When the Mg alloys melt contact with H13 steel, the presence of Cr has a suppression effect on the dissolution of Fe in melt. It is seen that the dissolution of Cr in the Mg alloys is quite small, around 10–20 ppm, if the low holding temperature and limited holding time is used. There is little specific study on the Cr influence on the corrosion properties of Mg alloys. Considering the comparable low chemical potential of Cr than Fe and Ni (−0.913 V vs −0.447 and −0.257 V), the Cr addition on the corrosion property of Mg alloys may be mildly comparable. There is almost no Ni presented in H13 steel. Therefore, H13 steel is recommended as a tooling steel for the melting process of Mg alloys combined with low melting temperature and limited melting time. Of course, more investigations on the effect of Cr on the properties and performance of Mg alloys are needed.

Because of the quite limited content (less than 0.1 wt%) of these impurities in alloys obtained in this work, the identification of the impurities-containing precipitates in the final solidified alloys by normal metallographic analysis approaches, such as XRD and EDS analysis, is difficult. The possible final states of the impurities in the alloys were calculated according

to the Scheil simulation using thermodynamic databases TCMG5 or COST507. According to our measured results, as shown in **Table 4**, the typical content of the impurities in the alloys was taken for calculations as an example. The content in the α(Mg) phase did not change much with limited varied compositions and impurities content (still in ppm order of magnitude), and possible precipitates containing excess impurities were listed. Of course, the types of precipitates also depend on the holding temperature, casting temperature, and casting condition (cooling rate). When no Ni is presented in the melt of AZ91 and AM50A, the precipitated phase containing impurities are mainly Al-Mn-(Fe) compounds. When there is a small amount of Ni presented in the melt, Al_3Ni compounds can be formed in the Al-containing Mg alloys. Cr is probably still presented as α(Cr) in the final solidified alloys (There is no literature information about the Cr-presented state in the solidified Mg alloys and because of the quite limited Cr content involved in this work, the micrographic analysis on the Cr distribution in alloys is difficult).

5. Conclusions

The amounts of impurities (Fe, Cr, Ni) in molten AZ91D and AM50A after holding them in contact with H13 steel, High-CrNi steel, and 20# steel for different periods in the temperature range of 650–780 °C were studied. Results show that

Table 3. The impurities content in the molten Mg alloys.

System		Reaction conditions		Impurity in melt [ppm in weight fraction]				
alloy	steel	T [°C]	Time [h]	Fe	Cr	Ni	Total	
AZ91D	20#	650	6	120	–	–	120	This work
		720	6	189	–	–	189	
		780	6	230	–	–	230	
AM50A	20#	650	6	100	–	–	100	
		720	6	123	–	–	123	
		780	6	179	–	–	179	
AZ91D	H13	650	6	79	20	–	90	
		720	6	150	15	–	165	
		780	6	170	27	–	197	
AM50A	H13	650	6	39	6	–	45	
		720	6	107	17	–	124	
		780	6	131	26	–	157	
AZ91D	High-CrNi	650	6	58	14	34	106	
		720	6	149	39	38	226	
		780	6	223	105	71	399	
AM50A	High-CrNi	650	6	46	5	20	71	
		720	6	102	35	65	202	
		780	6	134	67	131	332	
Pure Mg	Low-carbon	800	24	1200	–	–	1200	Taninouchi et al.[25]
		900	24	2000	–	–	2000	
		1000	24	4400	–	–	4400	
	SUS316	800	24	980	210	1300	2490	
		900	24	1800	660	5600	8060	
		1000	24	3600	1300	18 000	22 900	

Table 4. The distribution and state of the impurities in the solidified Mg alloys.

Mg alloys[a]	Scheil solidify temperature	Impurities content in whole alloy [ppm]			The state and distribution of impurities in solidified state			
		Fe	Cr	Ni	Content in α(Mg)[ppm]			Possible impurities-containing precipitates
					Fe	Cr	Ni	
AM50A	436 °C	150	–	–	<1	–	–	Al$_4$Mn
–	–	100	–	50	<1	<1	22	Al$_4$Mn, Al$_3$Ni
–	–	–	50	–	–	<1	–	α (Cr)
AZ91D	365 °C	150	–	–	<1	–	–	Al$_4$Mn
–	–	100	50	–	<1	–	1	Al$_4$Mn, Al$_3$Ni
–	–	–	50	–	–	<1	–	α (Cr)

[a]Tip: The data of Cr content in α(Mg) is from Mg–Cr system in COST507 database.

the amounts of impurities in the melt are correlated with multi-factors: 1) Fe content increases significantly in molten Mg alloys with elevated holding temperatures. Therefore, the melting of Mg alloys should be set to low temperature as long as it is compatible to other industrial requirements. 2) Amounts of dissolved Fe in molten AM50A are constantly smaller than those in molten AZ91D after similar treatments. This is attributed to the higher Mn content in AM50A (0.41Mn) than that in

AZ91D (0.22 Mn). 3) Fe content in the molten Mg alloys reached stable values in 1 h with the applied conditions in this work. In contrast, Cr and Ni content kept increasing after 6 h diffusion time in high temperature, probably due to their low content in the steels. 4) The presence of Cr in the steels can inhibit the dissolution of Fe into molten Mg alloys, but Ni can dissolve into the molten Mg alloys and severely deteriorate the corrosion resistance. Therefore, High-CrNi

steel (022Cr25Ni7Mo4N in the current work) is not recommended for using as tooling materials for molten Mg alloys. Consequently, H13 steel with certain Cr content and no Ni content is considered to be the most suitable tooling materials for molten Mg alloys among currently investigated steels.

Acknowledgements

Conflict of Interest

The authors declare no conflict of interest.

Keywords

[1] J. P. Weiler, *J. Magnes. Alloy* **2019**, *7*, 297.
[2] X. Wang, D. Xu, R. Wu, X. Chen, Q. Peng, L. Jin, Y. Xin, Z. Zhang, Y. Liu, X. Chen, G. Chen, K. Deng, H. Wang, *J. Mater. Sci. Technol.* **2018**, *34*, 245.
[3] W. J. Joost, P. E. Krajewski, *Scr. Mater.* **2017**, *128*, 107.
[4] T. C. Xu, Y. Yang, X. D. Peng, J. F. Song, F. S. Pan, *J. Magnes. Alloy* **2019**, *7*, 536.
[5] N. Mo, Q. Y. Tan, M. Bermingham, Y. D. Huang, H. Dieringa, N. Hort, M. X. Zhang, *Mater. Design* **2018**, *155*, 422.
[6] A. Atrens, G. Song, M. Liu, Z. Shi, F. Cao, M. S. Dargusch, *Adv. Eng. Mater* **2015**, *17*, 400.
[7] A. Atrens, S. Johnston, Z. Shi, M. S. Dargusch, *Scr. Mater.* **2018**, *154*, 92.
[8] A. Atrens, G. Song, F. Cao, Z. Shi, P. K. Bowen, *J. Magnes. Alloy* **2013**, *1*, 177.
[9] J. E. Hills, *SAE* **1983**, 830523.
[10] M. Liu, P. J. Uggowitzer, A. V. Nagasekhar, P. Schmutz, M. Easton, G. Song, A. Atrens, *Corros. Sci.* **2009**, *51*, 602.
[11] M. Liu, P. J. Uggowitzer, P. Schmutz, A. Atrens, *JOM* **2008**, 60.
[12] X. Chen, F. Pan, J. Mao, Z. Zhang, *J. Wuhan Univ. Technol.* **2013**, *28*, 1207.
[13] F. Pan, J. Mao, X. Chen, J. Peng, J. Wang, *Trans. Nonferrous Met. Soc. China* **2010**, *20*, 1299.
[14] X. Chen, F. Pan, J. Mao, J. Huang, *J. Mater. Sci.* **2011**, *47*, 514.
[15] X. Chen, J. Mao, F. Pan, J. Peng, J. Wang, *Trans. Nonferrous Met. Soc. China* **2010**, *20*.
[16] G. Song, A. Atrens, *Adv. Eng. Mater* **2003**, *5*, 837.
[17] J. Dai, B. Jiang, C. Peng, F. Pan, *J. Alloys Compd.* **2017**, *710*, 260.
[18] T. Haitani, Y. Tamura, T. Motegi, N. Kono, H. Tamehiro, *Mater. Sci. Forum* **2003**, *419–422*, 697.
[19] C. Scharf, A. Ditze, *Adv. Eng. Mater* **2007**, *9*, 566.
[20] T. Haitani, Y. Tamura, T. Motegi, N. Kono, H. Tamehiro, E. Sato, *J. Japan Inst. Light Metals* **2002**, *52*, 591.
[21] J. I. Kim, H. N. Nguyen, B. S. You, Y. M. Kim, *Scr. Mater.* **2019**, *162*, 355.
[22] A. Prasad, P. J. Uggowitzer, Z. Shi, A. Atrens, *Adv. Eng. Mater* **2012**, *14*, 477.
[23] J. Liu, T. Chen, Y. Yuan, J. Wu, L. Yang, A. Tang, D. Li, F. Pan, in *Magnesium Technology* (Eds: J. B. Jordon, V. Miller, V. V. Joshi, N. R. Neelameggham), Springer, Basel, Switzerland **2020**, pp. 55–59.
[24] F. Pan, X. Chen, T. Yan, T. Liu, J. Mao, W. Luo, Q. Wang, J. Peng, A. Tang, B. Jiang, *J. Magnes. Alloy* **2016**, *4*, 8.
[25] Y. K. Taninouchi, K. Nose, T. H. Okabe, *Metall. Mater. Trans. B* **2018**, *49*, 3432.
[26] J. O. Andersson, T. Helander, L. Höglund, P. Shi, B. Sundman, *Calphad*, **2002**, *26*, 273.
[27] S. Chen, W. Cao, C. Zhang, J. Zhu, F. Zhang, Q. Li, J. Zhang, *Calphad* **2016**, *55*, 63.
[28] Q. Luo, C. Zhai, D. Sun, W. Chen, Q. Li, *J. Mater. Sci. Technol.* **2019**, *35*, 2115.
[29] Q. Luo, Y. Guo, B. Liu, Y. Feng, J. Zhang, Q. Li, K. Chou, *J. Mater. Sci. Technol.* **2020**, *44*, 171.
[30] M. Venkatraman, J. P. Neumann, *Bull. Alloy Phase Diagrams* **1985**, *6*, 335.
[31] H. Okamoto, *J. Phase Equilib.* **2000**, *21*, 209.
[32] I. Ansara, A. Dinsdale, M. Rand, *Thermochemical Database for Light Metal Alloys*, Office for Official Publications of the European Communities, Luxembourg **1998**.
[33] A. A. Nayeb-Hashemi, J. B. Clark, *Bull. Alloy Phase Diagrams* **1985**, *6*, 164.
[34] C. He, Y. Du, H. L. Chen, H. W. Ouyang, *Int. J. Mater. Res.* **2008**, *99*, 907.
[35] K. N. Reichek, K. J. Clark, J. E. Hillis, *SAE* **1985**, 850417.
[36] W. Liu, Q. Gu, B. Liu, B. Wang, Q. Luo, J. Zhang, Y. Wang, Q. Li, *Mater. Charact.* **2018**, *145*, 135.
[37] W. Xu, L. Wei, Z. Zhang, Y. Liu, K.-C. Chou, H. Fan, Q. Li, *J. Alloys Compd.* **2019**, *784*, 859.
[38] P. Wang, J. Zhao, Y. Du, H. Xu, T. Gang, J. Fen, L. Zhang, C. He, S. Liu, H. Ouyang, *Int. J. Mater. Res.* **2011**, *102*, 6.
[39] M. Liu, P. J. Uggowitzer, A. V. Nagasekhar, P. Schmutz, M. Easton, G. L. Song, A. Atrens, *Corros. Sci.* **2009**, *51*, 602.
[40] G. Song, A. Atrens, *Adv. Eng. Mater* **1999**, *1*, 11.
[41] H. S. Tathgar, *Thesis*, University of Science and Technology **2001**.
[42] A. Froats, T. K. Aune, D. Hawke, W. Unsworth, J. E. Hillis, *ASM Int. Mater. Park* **1987**, 13.